DOI: 10.1002/chem.201000211

Syntheses and Characterization of $(C_2F_5)_3BCO$ and $(C_3F_7)_3BCO$

Michael Gerken,*[a, b] Gottfried Pawelke,[a] Eduard Bernhardt,[a] and Helge Willner[a]

Abstract: The new tris(perfluoroalkyl)-borane carbonyls, $(C_2F_5)_3BCO$ and $(C_3F_7)_3BCO$, were prepared by means of a novel synthetic route using commercially available precursors by reacting $K[(C_2F_5)_3BCOOH]$ and $K[(C_3F_7)_3BCOOH]$ with concentrated sulfuric acid in the last step. The carboxylic acids, $K[(C_2F_5)_3BCOOH]$ and $K[(C_3F_7)_3BCOOH]$, were prepared by oxidative cleavage of the C≡C triple bonds in $Cs[(C_2F_5)_3BC{\equiv}CPh]$ and $Cs[(C_3F_7)_3BC{\equiv}CPh]$ in a two-step process to yield $K[(C_2F_5)_3BCO{-}COPh]$ and $K[(C_3F_7)_3BCO{-}COPh]$ as isolable intermediates. Crystal structures were obtained of $K[(C_2F_5)_3BCO{-}COPh]$, $K[(C_2F_5)_3BCOOH]{\cdot}H_2O$, $(C_2F_5)_3BCO$, $K[(C_3F_7)_3BCOOH]\cdot 2H_2O$, and $(C_3F_7)_3BCO$. In the crystal structures of $(C_2F_5)_3BCO$ and $(C_3F_7)_3BCO$ the C≡O bond lengths are 1.109(2) and 1.103(5) Å, respectively, which are among the shortest observed to date. Tris(pentafluoroethyl)borane carbonyl and $(C_3F_7)_3BCO$ slowly decompose at room temperature to yield CO, difluoroperfluoroalkylboranes and perfluoroalkenes. The decomposition of $(C_2F_5)_3BCO$ was found to follow a first-order rate law with $E_a = 107\ kJ\,mol^{-1}$.

Keywords: boranes · carbonyl ligands · structure elucidation · vibrational spectroscopy

Introduction

Synthesis of the first tris(perfluoroalkyl)borane carbonyl, $(CF_3)_3BCO$, had been reported in 2002 by solvolysis of the $[B(CF_3)_3]^-$ ion in concentrated sulfuric acid [Eq. (1)].[1,2]

$$[B(CF_3)_4]^-_{(solv)} + H_3O^+ \xrightarrow[\text{conc. } H_2SO_4]{25\,^\circ C} (CF_3)_3BCO_{(g)} + 3\,HF_{(solv)} \quad (1)$$

Its high CO stretching frequency at 2252 cm^{-1} reflects the σ-bonding character of the CO group at the boron atom and the absence of any π backbonding. Tris(trifluoromethyl)borane carbonyl was subsequently shown to have diverse chemistry.[3] The chemistry of boranes and borates with longer perfluoroalkyl chains has been investigated less than that of boranes and borates with the trifluoromethyl group.[4] Boron compounds with longer perfluoroalkyl chains are expected to be more stable than trifluoromethyl derivatives, because B–CF_3 groups can easily eliminate CF_2. This has been exemplified by the instability of CF_3BF_2, whereas $C_2F_5BF_2$ is isolable.[5]

Therefore, the goal of the present study was the synthesis of tris(perfluoroalkyl)borane carbonyls with longer perfluoroalkyl chains and the comparison of their properties with those of the trifluoromethyl derivative.

Results and Discussion

Syntheses and properties of starting materials: The synthetic route to $(C_2F_5)_3BCO$ by means of solvolysis in concentrated sulfuric acid in analogy to Equation (1), was not possible because the hypothetical starting material, $[(CF_3)B(C_2F_5)_3]^-$, is still unknown. As a consequence, a new synthetic route had to be developed. Homologous $(CF_3)_3BCO$ has been shown to reversibly add H_2O at the carbonyl carbon atom to form the strong acid, $[H_3O][(CF_3)_3BCOOH]$, in solution and to lose H_2O upon drying [Eq. (2)].[2]

[a] Prof. Dr. M. Gerken, Dr. G. Pawelke, Dr. E. Bernhardt, Prof. Dr. H. Willner
Bergische Universität Wuppertal
FB C- Anorganische Chemie
Gaussstrasse 20, 42097 Wuppertal (Germany)

[b] Prof. Dr. M. Gerken
Permanent address: University of Lethbridge
Department of Chemistry and Biochemistry
Lethbridge, AB, T1K3M4 (Canada)
Fax: (+1) 403-329-2057
E-mail: michael.gerken@uleth.ca

Supporting information for this article is available on the WWW under http://dx.doi.org/10.1002/chem.201000211.

$$(CF_3)_3BCO + 2\,H_2O \rightleftharpoons [H_3O]^+[(CF_3)_3BCOOH]^- \quad (2)$$

Therefore, we investigated ways of synthesizing salts containing the $[(C_2F_5)_3BCOOH]^-$ ion, which was expected to form the desired carbonyl $(C_2F_5)_3BCO$ upon treatment with concentrated H_2SO_4. A promising precursor for the synthesis of $K[(C_2F_5)_3BCOOH]$ was shown to be $Cs[(C_2F_5)_3BC{\equiv}CPh]$, which had been prepared previously by the reaction sequence in Equations (3a–e) by using commercially available starting materials. Passing the reacting mixture through a cation-exchange resin yielded the cesium salt in the final step.[6]

$$BCl_3 + 6\,HNMe_2 \rightarrow B(NMe_2)_3 + 3\,[H_2NMe_2]Cl \quad (3a)$$

$$B(NMe_2)_3 + 2\,BBr_3 \rightarrow 3\,Br_2BNMe_2 \quad (3b)$$

$$Br_2BNMe_2 + 3\,C_2F_5I + 3\,P(NEt_2)_3 \rightarrow [(C_2F_5)_3BNMe_2]^- + 3\,[P(NEt_2)_3I]^+ + 2\,Br^- \quad (3c)$$

$$[(C_2F_5)_3BNMe_2]^- + CH_3I \rightarrow (C_2F_5)_3BNMe_3 + I^- \quad (3d)$$

$$(C_2F_5)_3BNMe_3 + HC{\equiv}CPh \xrightarrow[N(C_4H_9)_3]{185\,^\circ C} [HN(C_4H_9)_3][(C_2F_5)_3BC{\equiv}CPh] + NMe_3 \quad (3e)$$

Oxidative cleavage of the C≡C triple bond furnished the desired $[(C_2F_5)_3BCOOH]^-$ ion. Because the B–COOH bond must not be affected, a two-step process had to be utilized. In the first step, $Cs[(C_2F_5)_3BC{\equiv}CPh]$ was treated with a large excess of aqueous $KMnO_4$ at room temperature according to Equation (4).

$$3\,[(C_2F_5)_3BC{\equiv}CPh]^- + 2\,H_2O + 4\,MnO_4{}^- \rightarrow 3\,[(C_2F_5)_3BCO{-}COPh]^- + 4\,MnO_2 + 4\,OH^- \quad (4)$$

The reaction requires at least four days for completion because of the low solubility of $Cs[(C_2F_5)_3BC{\equiv}CPh]$ in water. Owing to the basic conditions, oxidation of the triple bond proceeds exclusively to $K[(C_2F_5)_3BCO\text{-}COPh]$ in high yield, if the temperature is kept at 25 °C. At higher temperatures, further oxidative cleavage takes place and considerable amounts of $[(C_2F_5)_3BOH]^-$ are formed. Like other 1,2-dicarbonyl compounds, ethanol solutions of $K[(C_2F_5)_3BCO\text{-}COPh]$ are yellow with absorptions at $\lambda = 403$ nm ($\varepsilon_1 = 55\ cm^{-1}\,L\,mol^{-1}$) and 333 nm ($\varepsilon_2 = 115\ cm^{-1}\,L\,mol^{-1}$). However, in the solid state, the yellow color almost disappears, depending on the cation. The potassium salt is still pale yellow, whereas the Cs^+ salt is almost colorless. The selective oxidative cleavage of the C–C bond of the dicarbonyl group was achieved by using excess hypobromite [Eq. (5)].

$$[(C_2F_5)_3BCO{-}COPh]^- + OBr^- + H_2O \rightarrow [(C_2F_5)_3BCOOH]^- + PhCOOH + Br^- \quad (5)$$

The benzoic acid, which is formed in equimolar amounts, was separated by extraction from an acidified solution using $CHCl_3$, because $K[(C_2F_5)_3BCOOH]$ is almost insoluble under these conditions. The $K[(C_2F_5)_3BCOOH]$ salt is a colorless solid and a weak acid in aqueous solutions with $pK_a = 8.0$ [Eq. (6)], which is significantly weaker than $[(CF_3)_3BCOOH]^-$ ($pK_a = 7.0$).[2] The $[(C_2F_5)_3BCO_2]^{2-}$ is less effectively solvated by water than $[(CF_3)_3BCO_2]^{2-}$ as a consequence of the increasing hydrophobicity with increasing length of the perfluoroalkyl group.

$$[(C_2F_5)_3BCOOH]^- + H_2O \rightleftharpoons H_3O^+ + [(C_2F_5)_3BCO_2]^{2-} \quad (6)$$

The monohydrate, $K[(C_2F_5)_3BCOOH]{\cdot}H_2O$, precipitates from aqueous solution. Single crystals were grown from a mixture of diethyl ether and CH_2Cl_2 and were structurally characterized by using X-ray diffraction (vide infra). Analysis of DSC measurements reveals that the onset of the loss of water of hydration is at 62 °C and decomposition commences at 170 °C. The anhydrous $K[(C_2F_5)_3BCOOH]$ salt can easily be obtained at 50 °C under dynamic vacuum.

Synthesis and properties of $(C_2F_5)_3BCO$: Tris(pentafluoroethyl)borane carbonyl was prepared upon treatment of $K[(C_2F_5)_3BCOOH]$ with concentrated sulfuric acid with concomitant removal of $(C_2F_5)_3BCO$ under dynamic vacuum and trapping at −60 °C [Eq. (7)].

$$K[(C_2F_5)_3BCOOH] + H_2SO_4 \rightarrow (C_2F_5)_3BCO_{(g)} + KHSO_4 + H_2O \quad (7)$$

Tris(pentafluoroethyl)borane carbonyl is a colorless crystalline solid at −78 °C, which is stable under anhydrous conditions at that temperature. It melts at −28 °C and the boiling point of ≈107 °C was extrapolated from vapor pressure measurements. At 0 and 15 °C its vapor pressures are 3.7 and 10.5 mbar, respectively. Close to ambient temperature, $(C_2F_5)_3BCO$ decomposes to CO, $C_2F_5BF_2$, and 1-octafluorobutene, $F_2C{=}CF(C_2F_5)$ according to Equation (8).

$$(C_2F_5)_3BCO \rightleftharpoons (C_2F_5)_3B + CO \rightarrow C_2F_5BF_2 + F_2C{=}CF(C_2F_5) + CO \quad (8)$$

The gas-phase IR spectrum of a fully decomposed sample (see Figure S1 in the Supporting Information) contained bands at $\tilde{\nu} = 1790$, 1375, 1346, 1322, 1217, 1186, 946, 757, and 686 cm^{-1} corresponding to $F_2C{=}CF(C_2F_5)$,[7] bands at $\tilde{\nu} = 1517$, 1466, 1376, 1341, 1217, 1140, 1105, 990, 605, and 527 cm^{-1} corresponding to $C_2F_5BF_2$,[5] and a weak band at $\tilde{\nu} = 2143\ cm^{-1}$ arising from CO. Furthermore, the decomposition products were unambiguously identified by using ^{19}F NMR spectroscopy of a decomposed sample in CD_2Cl_2, giving rise to signals at $\delta = -86.0$ (CF_3), −88.2 ($FFC{=}$), −105.5 ($FFC{=}$), −122.7 (CF_2), and −191.8 ppm ($=CF$) for $F_2C{=}CF(C_2F_5)$[8] and $\delta = -76.2$ (BF_2), −84.6 (CF_3), and −134.7 ppm (CF_2) for $C_2F_5BF_2$.[5]

The first step of the decomposition can be assumed to be the slow B–CO bond dissociation. Based on a decomposition study of $(CF_3)_3BCO$,[5] the unstable super Lewis-acid

$(C_2F_5)_3B$ is expected to undergo a C–F→B–F fluoride shift to yield $(C_2F_5)_2BF(CFCF_3)$, followed by the migration of a pentafluoroethyl group and elimination of $F_2C{=}CF(C_2F_5)$. The decomposition of $(C_2F_5)_3BCO$ follows a first-order rate law with halflifes of 120, 62, 32, 15, and 8 min at 15, 20, 25, 30, and 35 °C, respectively. The Arrhenius plot (Figure 1)

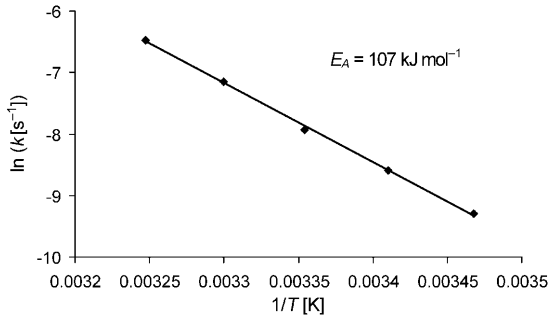

Figure 1. Arrhenius plot for the decomposition of $(C_2F_5)_3BCO$ (1st order).

gives an activation energy of $E_A = 107\ kJ\,mol^{-1}$, which is the same value within error limits as the activation energy for exchange between ^{13}CO and $(CF_3)_3BCO$ ($E_A = 112\ kJ\,mol^{-1}$). It has been noted that the activation energy for the B–CO bond cleavage is essentially identical with the B–CO bond energy. This bond cleavage is the rate-determining step in the decomposition of the tris(perfluoroalkyl)-borane carbonyls.

Synthesis and properties of $(C_3F_7)_3BCO$: Tris(heptafluoropropyl)borane carbonyl was prepared by a reaction sequence analogous to the synthesis of its pentafluoroethyl derivative, starting from $Cs[(C_3F_7)_3BC{\equiv}CPh]$, via $K[(C_3F_7)_3BCO{-}COPh]$ and $K[(C_3F_7)_3BCOOH]$. The intermediate, $K[(C_3F_7)_3BCO{-}COPh]$ was characterized by its ^1H, ^{11}B, ^{13}C, and ^{19}F NMR spectra and $K[(C_3F_7)_3BCOOH]$ by IR and ^{11}B, ^{13}C, and ^{19}F NMR spectroscopy. A pK_a value of 8.2 was determined for $[(C_3F_7)_3BCOOH]^-$, which fits in the series of $[(C_2F_5)_3BCOOH]^-$ (p$K_a = 8.0$) and $[(C_2F_5)_3BCOOH]^-$ (p$K_a = 7.0$) (vide supra). Similar to its pentafluoroethyl analogue, $K[(C_3F_7)_3BCOOH]$ is obtained as its dihydrate, as determined by X-ray crystallography (vide infra), which can be dehydrated under dynamic vacuum at 50 °C, as seen by IR spectroscopy. The carbonyl was generated by the reaction of $K[(C_3F_7)_3BCOOH]$ with concentrated sulfuric acid [Eq. (9)] and was trapped at −20 °C. The melting point of $(C_3F_7)_3BCO$ is 5 °C and its vapor pressure at 20 °C is approximately 1 mbar.

$$K[(C_3F_7)_3BCOOH] + H_2SO_4 \rightarrow (C_3F_7)_3BCO_{(g)} + KHSO_4 + H_2O \quad (9)$$

Tris(heptafluoropropyl)borane carbonyl decomposes at room temperature to CO, $C_3F_7BF_2$, and dodecafluorohexene, C_6F_{12} [Eq. (10)]. Analysis of the ^{19}F NMR spectra of the decomposed sample revealed the presence of a mixture of trans-2-dodecafluorohexene and trans-3-dodecafluorohexene. Compared to $(C_2F_5)_3BCO$, the higher homologue is more difficult to transfer by vacuum distillation because of its lower vapor pressure and its similar decomposition behavior. It is expected that the next homologue, $(C_4F_9)_3BCO$ would be even more difficult to prepare and to handle.

$$(C_3F_7)_3BCO \rightleftharpoons (C_3F_7)_3B + CO \rightarrow C_3F_7BF_2 + C_6F_{12} + CO \quad (10)$$

Vibrational spectroscopy: *$K[(C_2F_5)_3BCO{-}COPh]$, $K[(C_2F_5)_3BCOOH]{\cdot}H_2O$, $K[(C_2F_5)_3BCOOH]$, $K[(C_3F_7)_3BCOOH]{\cdot}2\,H_2O$, and $K[(C_3F_7)_3BCOOH]$*: Solid $K[(C_2F_5)_3BCO{-}COPh]$ and $K[(C_2F_5)_3BCOOH]$ were studied by IR and Raman spectroscopy and their vibrational spectra are depicted in Figures 2 and 3. The monohydrate $K[(C_2F_5)_3BCOOH]{\cdot}H_2O$ was studied by IR spectroscopy only (Figure 4). A Raman spectrum of $K[(C_2F_5)_3BCOOH]{\cdot}H_2O$ has not been obtained, since the sample loses its water of hydration upon irradiation by the Raman laser. The tris-

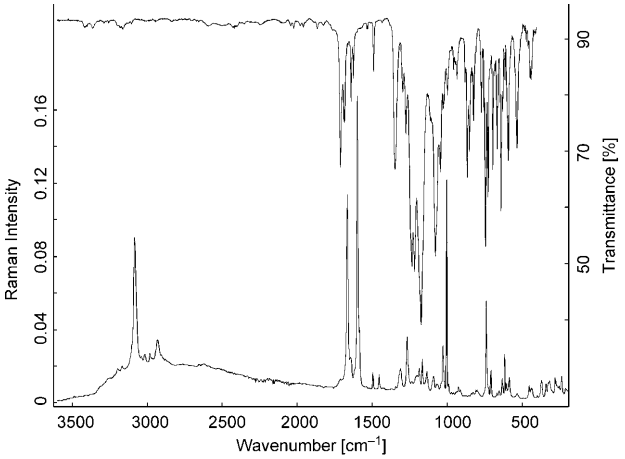

Figure 2. IR (upper trace) and Raman spectra (lower trace) of solid $K[(C_2F_5)_3BCOCOPh]$.

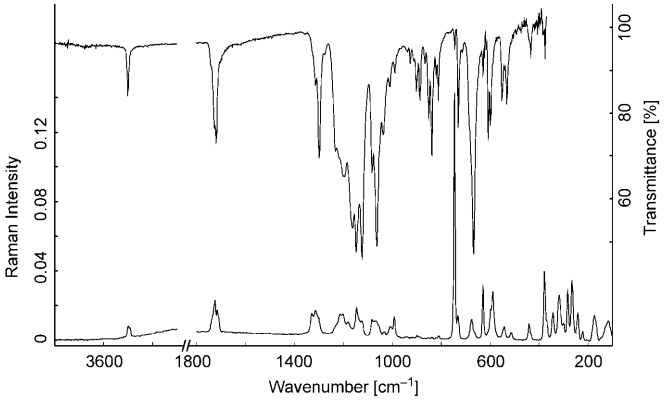

Figure 3. IR (upper trace) and Raman spectra (lower trace) of solid $K[(C_2F_5)_3BCOOH]$.

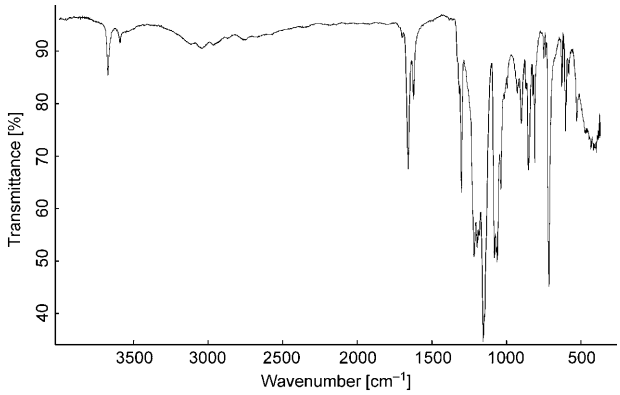

Figure 4. IR spectrum of solid K[$(C_2F_5)_3$BCOOH]·H_2O.

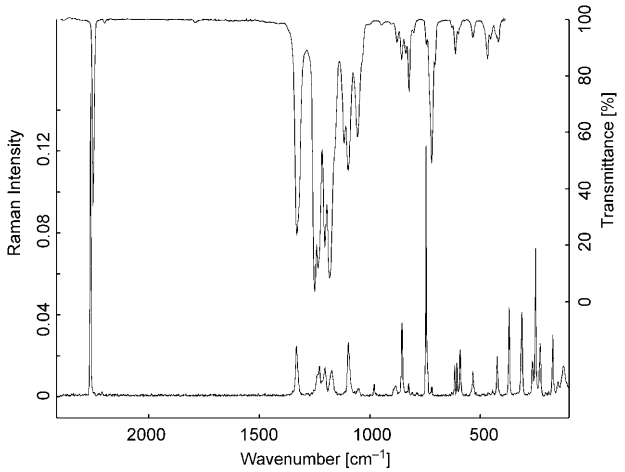

Figure 5. Gas-phase IR (upper trace) and low-temperature Raman spectra (lower trace) of $(C_2F_5)_3$BCO.

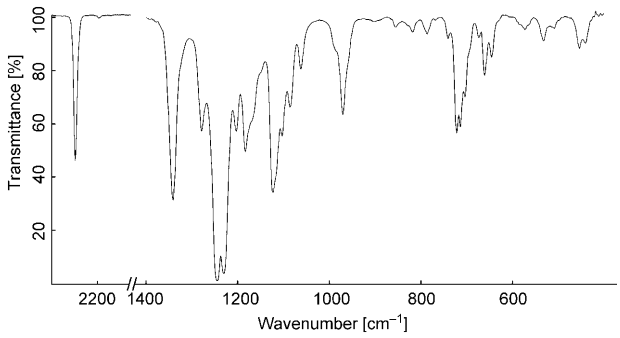

Figure 6. Gas-phase IR spectrum of $(C_3F_7)_3$BCO.

(heptafluoropropyl) species, K[$(C_3F_7)_3$BCOOH]·2 H_2O, and K[$(C_3F_7)_3$BCOOH] were characterized by IR spectroscopy (see Figure S2 in the Supporting Information).

The vibrational spectra of K[$(C_2F_5)_3$BCOOH]·H_2O, and K[$(C_2F_5)_3$BCOOH] exhibit marked differences, especially in the OH and CO stretching regions. For K-[$(C_2F_5)_3$BCOOH]·H_2O two IR bands were observed in the OH stretching region at $\tilde{\nu}=3671$ and 3589 cm^{-1} and two bands in the CO stretching region at $\tilde{\nu}=1659$ and 1623 cm^{-1}. This is in agreement with the X-ray crystallographic observation of two crystallographically different hydrogen-bridged dimers. The anhydrous sample, shows only one OH stretching band at $\tilde{\nu}=3500$ cm^{-1} and CO stretching bands at $\tilde{\nu}=1725$ and 1718 cm^{-1} in the IR spectrum. Similar wavenumbers were observed for the CO and OH stretching bands in the IR spectra of anhydrous K[$(C_3F_7)_3$BCOOH] and its dihydrate, which has been identified by X-ray crystallography. For example, while the CO stretching bands for the hydrate were observed at $\tilde{\nu}=1663$ and 1624 cm^{-1}, these bands are shifted to $\tilde{\nu}=1723$ and 1705 cm^{-1} for the anhydrous form. These similarities in their IR spectra suggest similar structural properties between the pentafluoroethyl and heptafluoropropyl species.

$(C_2F_5)_3$BCO and $(C_3F_7)_3$BCO: Gas-phase IR and low-temperature Raman spectra were recorded of $(C_2F_5)_3$BCO (Figure 5), and $(C_3F_7)_3$BCO was characterized by its gas-phase IR spectrum shown in Figure 6. The Raman spectrum of $(C_2F_5)_3$BCO is dominated by an intense CO stretching band and a band at $\tilde{\nu}=746$ cm^{-1} that has been assigned to the symmetric CF_3 deformation mode,[9] characteristic for perfluoroalkyl groups. The gas-phase CO stretching frequency of $(C_2F_5)_3$BCO ($\tilde{\nu}=2252$ cm^{-1}) and of $(C_3F_7)_3$BCO ($\tilde{\nu}=$ 2249 cm^{-1}) are almost the same as that of $(CF_3)_3$BCO ($\tilde{\nu}=$ 2252 cm^{-1}), suggesting that the bonding situation for the carbonyl groups is very similar in these three species and that the length of the perfluoroalkyl chain has little effect on the CO bonding.

NMR Spectroscopy: The ^{19}F and ^{11}B NMR spectra were recorded for K[$(C_2F_5)_3$BCO-COPh], K[$(C_2F_5)_3$BCOOH], $(C_2F_5)_3$BCO, K[$(C_3F_7)_3$BCO−COPh], K[$(C_3F_7)_3$BCOOH], and $(C_3F_7)_3$BCO. In addition, K[$(C_2F_5)_3$BCOOH], K-[$(C_3F_7)_3$BCOOH], and $(C_2F_5)_3$BCO were studied by ^{13}C and K[$(C_2F_5)_3$BCO−COPh] and K[$(C_3F_7)_3$BCO−COPh] were studied by ^{1}H and ^{13}C NMR spectroscopy. All NMR spectroscopic data are listed in Table 1.

The ^{19}F and ^{13}C NMR spectroscopic data for the perfluoroalkyl chains are found to be in the expected range. Three-bond ^{19}F–^{19}F coupling constants in perfluoroalkyl groups are usually very small (<1 Hz), and were, consequently, not observed. The ^{13}C resonance of the CO group in $(C_2F_5)_3$BCO ($\delta=160.3$ ppm) is similar to that of $(CF_3)_3$BCO ($\delta=$ 159.8 ppm).[2] Among our perfluoroethyl and perfluoropropyl borone compounds presented in this study, only the ^{11}B NMR spectra of the dicarbonyl salts, K[$(C_2F_5)_3$BCO−COPh] and K[$(C_3F_7)_3$BCO−COPh], were sufficiently narrow to show $^{2}J(^{11}B–^{19}F)$ couplings. In contrast to $[(CF_3)_3BCOOH]^-$, which gave rise to a sharp ^{11}B multiplet, the ^{11}B resonances of $[(C_2F_5)_3BCOOH]^-$ and $[(C_3F_7)_3BCOOH]^-$ are broadened and couplings to ^{19}F of the perfluoroalkyl chains were not resolved. The broadening of the ^{11}B resonances is a consequence of the larger electric field gradient (efg) about boron in the perfluoroethyl and

Table 1. NMR-spectroscopic data (δ in ppm, J in Hz) of K[$(C_2F_5)_3$BCO−COPh], K[$(C_2F_5)_3$BCOOH], $(C_2F_5)_3$BCO, K[$(C_3F_7)_3$BCO−COPh], K-[$(C_3F_7)_3$BCOOH], and $(C_3F_7)_3$BCO.

		[$(C_2F_5)_3$BCO−COPh]$^-$[a]	[$(C_3F_7)_3$BCO−COPh]$^-$[a]	($C_2F_5)_3$BCO	($C_3F_7)_3$BCO[b]	[$(C_2F_5)_3$BCOOH]$^-$[a]	[$(C_3F_7)_3$BCOOH][a]
^{1}H							
	δ (C_6H_5)	7.43/7.54/7.82	7.42/7.52/7.81				
^{19}F							
	δ (BCF_2C)	−114.8	−111.6	−114.0[c]	−113.0	−117.7	−113.8
	δ (CCF_2C)		−122.2		−124.5		−122.5
	δ (CF_3)	−81.3	−81.1	−82.1[c]	−83.4	−82.0	−81.0
^{11}B							
	δ (B)	−14.8	−14.1	−16.4[c]	−18.0	−16.9	−16.3
	^2J(^{11}B–^{19}F)	17.6	17.4				
^{13}C							
	δ (BCF$_2$C)	123	125	119.4[d]		123	125
	^1J(^{13}C–^{19}F)				256[e]		
	δ (CCF$_2$C)		112.8				112.9
	^1J(^{13}C–^{19}F)				249[e]		
	δ (CCF$_3$)	122.8	120.8	116.3[d]		122.6	120.8
	^1J(^{13}C–^{19}F)	286.0	289	284[d]	286[e]	286	288
	^2J(^{13}C–^{19}F)	33.3	38	33[d]		32	37
	δ (BCO)	236.1	235.3	160.3[d]		191	190
	^1J(^{11}B–^{13}C)	55.1	55			69	69
	δ (CCO)	198.0	197.3				
	^1J(^{11}B–^{13}C)	11.0	11				
	δ (C_6H_5)	135.2/134.3/131.0/129.6	135.4/134.2/131.1/129.6				

[a] In [D$_6$]acetone. [b] Neat liquid at −6 °C. [c] In a CH_2Cl_2/$CFCl_3$ mixture. [d] Neat liquid at −20 °C. [e] Observed in the ^{19}F NMR spectrum.

perfluoropropyl derivatives, resulting in faster quadrupolar relaxation rates compared to that of the trifluoromethyl species. The ^{11}B resonance for $(CF_3)_3$BCO was significantly broader than that of the corresponding carboxylate salt; however, ^2J(^{11}B–^{19}F) coupling was still resolved. For $(C_2F_5)_3$BCO and $(C_3F_7)_3$BCO, on the other hand, the ^{11}B resonances are broad singlets. The significant efg that causes an intermediate quadrupolar relaxation rate and a quadrupolar collapse of the multiplet is reflected by the fact that the local symmetry about boron deviates significantly from tetrahedral with one short B−CO bond and three longer B−CF_2 bonds as found in the crystal structure of $(C_2F_5)_3$BCO (vide infra). The line width of the ^{11}B resonance increases significantly with longer perfluoroalkyl groups, that is, $(C_2F_5)_3$BCO and $(C_3F_7)_3$BCO (neat liquids), have line widths of $\Delta\nu_{1/2}=350$ Hz; $\Delta\nu_{1/2}=680$ Hz, respectively. The line width for $(C_2F_5)_3$BCO in CH_2Cl_2/$CFCl_3$ solvent mixture is smaller with 96 Hz, which contain unresolved ^2J(^{19}F–^{11}B) coupling of the BCF_2 groups that are usually in the range of 17 to 18 Hz.[4] Fluorine-decoupling reduced the line width of the ^{11}B resonance of $(C_2F_5)_3$BCO in solution to 43 Hz. The increase in efg and, therefore, in the relaxation rate along this series of boron carbonyls is likely a consequence of symmetry lowering due to packing of the large perfluoroalkyl groups.

Of special interest is the ^{13}C resonance of the carboxylic group in [$(C_2F_5)_3$BCOOH]$^-$ at $\delta=191$ ppm, which is shifted to higher frequencies upon deprotonation to 197 ppm. This shift is typical of carboxylic acids; a similar shift is observed for acetic acid and the acetate anion (CH_3COOH: $\delta=178.1$ ppm; CH_3COO^-: $\delta=182.6$ ppm).[10] The observed value is at the upper limit of the scale for carboxylic acids and also significantly higher than that of [$(CF_3)_3$BCOOH]$^-$ at $\delta=186.4$ ppm, whereas the ^1J(^{11}B–^{13}C) coupling constants are almost the same with approximately 69 Hz.[2]

Crystal structures: Details of the data collection parameters and other crystallographic information for K[$(C_2F_5)_3$BCO−COPh], K[$(C_2F_5)_3$BCOOH]·H_2O, K[$(C_3F_7)_3$BCOOH]·2H_2O, $(C_2F_5)_3$BCO, and $(C_3F_7)_3$BCO are given in Table 2, and important bond lengths and angles are listed in Table 3.

Structure of K[$(C_2F_5)_3$BCO−COPh]: The potassium salt of [$(C_2F_5)_3$BCO−COPh]$^-$ crystallizes as two polymorphs in the monoclinic space groups, $P2_1/n$ and $I2/a$. The bond lengths and angles of the [$(C_2F_5)_3$BCO−COPh]$^-$ in the two polymorphic crystal structures are the same within 3σ. The structures differ mainly in the OCCO torsion angle ($P2_1/n$: 91.9(6)°, Figure 7; $I2/a$: 102.8(7)°). Since a disorder in one pentafluoroethyl group was observed for the $I2/a$ space group, only structural data for the ordered $P2_1/n$ structure are given in Table 3.

Structures of K[$(C_2F_5)_3$BCOOH]·H_2O and K-[$(C_3F_7)_3$BCOOH]·2H_2O: The hydrate of K[$(C_2F_5)_3$BCOOH] crystallizes in the monoclinic space group $P2_1/c$. The unit cell contains two crystallographic independent [$(C_2F_5)_3$BCOOH]$^-$, which form two hydrogen-bonded dimers with their respective symmetry-related counterparts (Figure 8). The oxygen of the water molecules bridge two potassium cations (see Figure S3 in the Supporting Information). The additional coordination sites about K(1) and K(2) are occupied by fluorine atoms of the pentafluoroethyl groups and oxygen atoms from the carboxylic acid groups, resulting in coordination numbers of eight and nine for K(1) and K(2), respectively. The dihydrate of K[$(C_3F_7)_3$BCOOH]

Table 2. Crystallographic data for $K[(C_2F_5)_3BCO{-}COPh]$, $K[(C_2F_5)_3BCOOH]\cdot H_2O$, $K[(C_3F_7)_3BCOOH]\cdot 2H_2O$, $(C_2F_5)_3BCO$, and $(C_3F_7)_3BCO$.

	$K[(C_2F_5)_3BCO{-}COPh]$[a]	$K[(C_2F_5)_3BCO{-}COPh]$[b]	$K[(C_2F_5)_3BCOOH]\cdot H_2O$[c]	$K[(C_3F_7)_3BCOOH]\cdot 2H_2O$[d]	$(C_2F_5)_3BCO$[e]	$(C_3F_7)_3BCO$[f]
formula	$C_{14}H_5BF_{15}KO_2$	$C_{14}H_5BF_{15}KO_2$	$C_7H_3BF_{15}KO_3$	$C_{10}H_5BF_{21}KO_4$	$C_7BF_{15}O$	$C_{10}BF_{21}O$
fw [g mol^{-1}]	540.09	540.09	470.00	638.05	395.88	545.91
T [K]	150	300	150	150	150	150
color	colorless	colorless	colorless	colorless	colorless	colorless
crystal size [mm^3]	0.223×0.123 ×0.097	0.40×0.26 ×0.12	0.206×0.093 ×0.042	0.188×0.169 ×0.071	0.249×0.159 ×0.048	0.234×0.051 ×0.039
crystal system	monoclinic	monoclinic	monoclinic	triclinic	monoclinic	hexagonal
space group	$P2_1/n$	$I2/a$	$P2_1/c$	$P\bar{1}$	$P2_1/c$	$P6_3$
a [Å]	8.2821(3)	24.3897(14)	7.7540(3)	11.1192(3)	12.3491(4)	10.2405(7)
b [Å]	22.5262(7)	8.4292(5)	19.3634(10)	18.0314(7)	16.9011(4)	10.2405(7)
c [Å]	9.5913(3)	19.0502(11)	19.3003(8)	22.0823(6)	12.8111(4)	9.0985(9)
α [°]	90	90	90	106.592(3)	90	90
β [°]	90.271(3)	103.303(1)	94.232(4)	92.770(2)	115.493(4)	90
γ [°]	90	90	90	107.053(3)	90	120
volume [Å^3]	1789.35(10)	3811.4(4)	2889.9(2)	4014.1(2)	2413.51(13)	826.31(11)
Z	4	8	8	8	8	2
ρ_{calcd} [mg m^{-3}]	2.005	1.882	2.161	2.112	2.179	2.194
R_1[g] [$I>2\sigma(I)$]	0.0335	0.0812	0.0389	0.0846	0.0327	0.0383
R_1[g] (all)	0.0425	0.0905	0.0678	0.1210	0.0615	0.0611
wR_2[h] [$I>2\sigma(I)$]	0.0870	0.1736	0.0846	0.2400	0.0731	0.0892
wR_2[h] (all)	0.0899	0.1787	0.0888	0.2554	0.0787	0.0950
largest diff. peak/hole [e Å^{-3}]	0.628/−0.342	0.505/−0.415	0.518/−0.478	1.678/−1.087	0.316/−0.368	0.356/−0.228

[a] CCDC-763012. [b] CCDC-763014. [c] CCDC-763009. [d] CCDC-763011. [e] CCDC-763010. [f] CCDC-763013. [g] R_1 is defined as $\Sigma||F_o|-|F_c||/\Sigma|F_o|$. [h] wR_2 is defined as $[\Sigma[w(F_o^2-F_c^2)^2]/\Sigma w(F_o^2)^2]^{1/2}$.

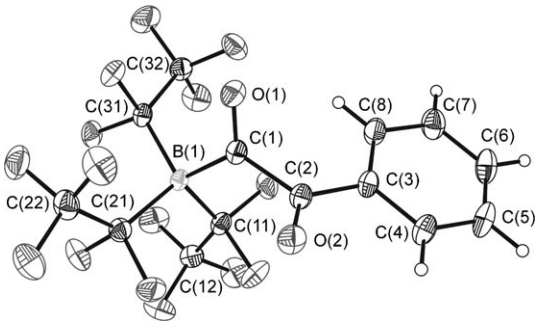

Figure 7. View of the $[(C_2F_5)_3BCO{-}COPh]^-$ ion in the X-ray crystal structure of $K[(C_2F_5)_3BCO{-}COPh]$ ($P2_1/n$ polymorph). Thermal ellipsoids are drawn at the 50% probability level.

crystallizes in the triclinic space group $P\bar{1}$ with four crystallographically independent anion molecules in the unit cell. All $[(C_3F_7)_3BCOOH]^-$ ions form dimers and the water molecules are found to coordinate to the K^+ ions, in a bridging and terminal fashion (see Figure S4 in the Supporting Information). The K^+ ions in $K[(C_3F_7)_3BCOOH]\cdot 2H_2O$ have coordination numbers of nine and ten. Several heptafluoropropyl side chains and two water molecules exhibit variable degrees of disorder. Especially the heptafluoropropyl groups that were not fixed by coordination to the K^+ cations exhibit disorder. One $[(C_3F_7)_3BCOOH]^-$ was found to be essentially ordered (see Figure S5 in the Supporting Information).

Dimer formation is a general feature observed for carboxylic acids. However, the formation of dimers found for the $[(C_2F_5)_3BCOOH]^-$ and $[(C_3F_7)_3BCOOH]^-$ carboxylic acid anions is noteworthy. This is possible, as the ionic charge of the borate anions is sufficiently diffuse to allow close interactions between the two anions. Although one

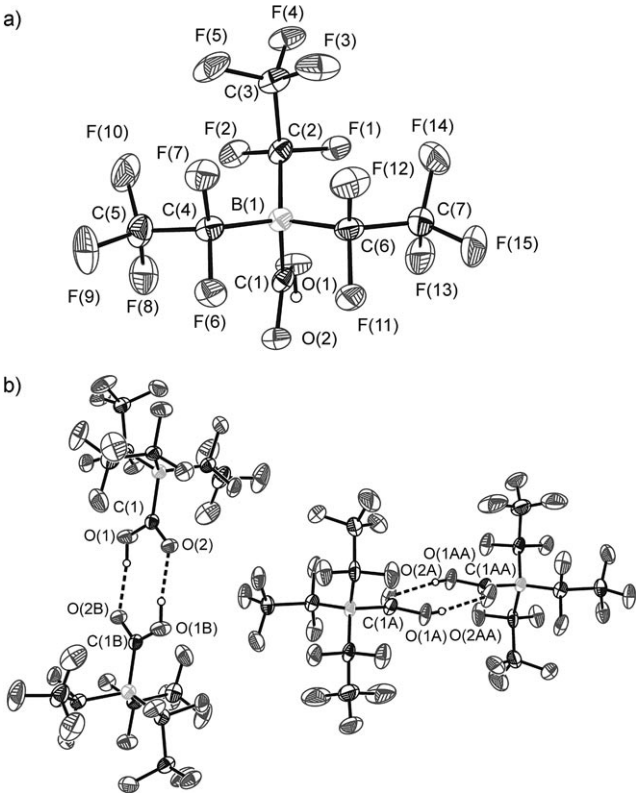

Figure 8. a) Structure of the $[(C_2F_5)_3BCOOH]^-$ ion in the crystal structure of $K[(C_2F_5)_3BCOOH]\cdot H_2O$ and b) dimers of $[(C_2F_5)_3BCOOH]^-$. Thermal ellipsoids are drawn at the 50% probability level.

$[(C_2F_5)_3BCOOH]^-$ contains one short B–COOH bond (1.637(3) Å) and three longer B–CF_2 bond (1.652(3)–1.659(3) Å), surprisingly the shortest B–C bond in the

Table 3. Selected bond lengths and angles for K[$(C_2F_5)_3$BCO−COPh] ($P2_1/n$), K[$(C_2F_5)_3$BCOOH]·H_2O, $(C_2F_5)_3$BCO, and $(C_3F_7)_3$BCO.[a]

K[$(C_2F_5)_3$BCO−COPh] ($P2_1/n$)			
Bond lengths and contacts [Å]			
C(1)−O(1)	1.225(2)	C(2)−O(2)	1.221(2)
C(1)−C(2)	1.549(2)	B(1)−C(1)	1.668(2)
B(1)−C(11)	1.656(2)	B(1)−C(21)	1.652(2)
B(1)−C(31)	1.652(2)		
Bond angles [°]			
C(1)-B(1)-C(11)	106.43(12)	C(1)-B(1)-C(21)	110.27(12)
C(1)-B(1)-C(31)	108.35(13)	B(1)-C(1)-O(1)	123.66(14)
B(1)-C(1)-C(2)	124.09(13)	O(1)-C(1)-C(2)	112.15(14)
C(1)-C(2)-O(2)	116.05(14)	C(1)-C(2)-C(3)	119.44(14)
O(2)-C(2)-C(3)	124.34(15)		
K[$(C_2F_5)_3$BCOOH]·H_2O			
Bond lengths and contacts [Å]			
C(1)−O(1)	1.325(3)	C(1A)−O(1A)	1.293(3)
C(1)−O(2)	1.235(3)	C(1A)−O(2A)	1.266(3)
B(1)−C(1)	1.637(3)	B(1A)−C(1A)	1.653(3)
B(1)−C(2)	1.652(3)	B(1A)−C(2A)	1.650(3)
B(1)−C(4)	1.656(3)	B(1A)−C(4A)	1.637(4)
B(1)−C(6)	1.659(3)	B(1A)−C(6A)	1.659(3)
H(1)···O(2)^{i}	1.80(3)	H(2)···O(1)^{ii}	2.05(3)
O(1)···O(2)^{i}	2.670(2)	O(2)···O(1)^{ii}	2.721(2)
K(1)−O(1S)	2.798(2)	K(2)−O(2S)	2.7242(19)
K(1)−O(1S)^{iii}	2.7995(18)	K(2)−O(2S)^{iv}	2.788(2)
K(1)−O(2)	2.7509(15)	K(2)−O(1A)^{v}	2.8117(18)
K(1)−F(6)	2.8202(14)	K(2)−F(1A)	2.7985(14)
K(1)−F(11)	2.8295(14)	K(2)−F(7A)^{v}	2.6634(13)
K(1)−F(5A)	2.8191(14)	K(2)−F(3)^{vi}	2.7959(16)
K(1)−F(11A)	2.8665(14)	K(2)−F(12)^{vi}	2.8766(16)
K(1)−F(1)^{iii}	2.6462(14)	K(2)−F(7)^{vi}	3.0942(16)
		K(2)−O(2A)	3.3799(19)
Bond angles [°]			
B(1)-C(1)-O(1)	117.9(2)	B(1A)-C(1A)-O(1A)	118.2(2)
O(1)-C(1)-O(2)	119.2(2)	O(1A)-C(1A)-O(2A)	119.3(2)
C(1)-B(1)-C(2)	108.8(2)	C(1A)-B(1A)-C(2A)	106.2(2)
C(1)-B(1)-C(4)	108.3(2)	C(1A)-B(1A)-C(4A)	110.5(2)
C(1)-B(1)-C(6)	106.3(2)	C(1A)-B(1A)-C(6A)	106.2(2)
O(1)-H(1)···O(2)^{i}	173(3)	O(2)-H(2)···O(1)^{ii}	174(4)
$(C_2F_5)_3$BCO			
Bond lengths [Å]			
C(1)−O(1)	1.109(2)	C(1A)−O(1A)	1.109(2)
B(1)−C(1)	1.618(2)	B(1A)−C(1A)	1.625(2)
B(1)−C(2)	1.643(2)	B(1A)−C(2A)	1.638(2)
B(1)−C(4)	1.644(2)	B(1A)−C(4A)	1.640(3)
B(1)−C(6)	1.634(3)	B(1A)−C(6A)	1.644(2)
Bond angles [°]			
B(1)-C(1)-O(1)	178.09(16)	B(1A)-C(1A)-O(1A)	179.54(19)
C(1)-B(1)-C(2)	104.27(12)	C(1A)-B(1A)-C(2A)	104.87(13)
C(1)-B(1)-C(4)	107.03(13)	C(1A)-B(1A)-C(4A)	105.73(12)
C(1)-B(1)-C(6)	104.43(13)	C(1A)-B(1A)-C(6A)	104.63(13)
$(C_3F_7)_3$BCO			
Bond lengths [Å]			
C(1)−O(1)	1.105(5)	B(1)−C(1)	1.638(5)
B(1)−C(2)	1.660(3)		
Bond angles [°]			
B(1)-C(1)-O(1)	180.000(2)	C(1)-B(1)-C(2)	106.7(3)

[a] Atom generated by symmetry operation: i: $-x$, $-y+1$, $-z+1$; ii: $-x+1$, $-y+1$, $-z+2$; iii: $-x+1$, $-y+1$, $-z+1$; iv: $-x$, $-y+1$, $-z+2$; v: $x-1$, y, z; vi: $-x$, $y+1/2$, $-z+3/2$.

second crystallographically independent anion links one pentafluoroethyl group to boron (1.637(4) Å). Besides packing effects, this difference may be a consequence of the different strengths of hydrogen bonding found in the two different dimers.

Structure of $(C_2F_5)_3BCO$: Tris(pentafluoroethyl)borane carbonyl crystallizes in the monoclinic space group $P2_1/c$ with two crystallographically independent molecules in the unit cell. The bond lengths and angles in both molecules are very similar. Both $(C_2F_5)_3$BCO molecules adopt approximate C_3 symmetry in the crystal structure with essentially linear BCO moieties and propeller-like arrangements of the three pentafluoroethyl groups (Figure 9). The low-temperature

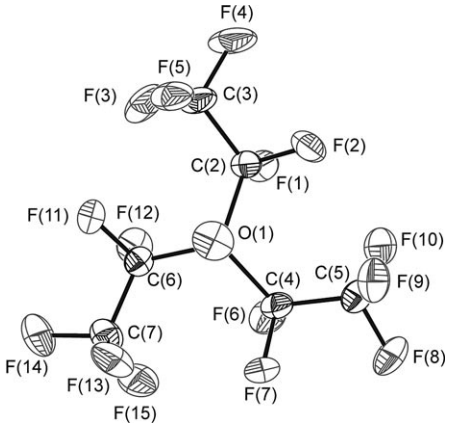

Figure 9. View along the BCO axis of one of the two crystallographically independent molecules in the X-ray crystal structure of $(C_2F_5)_3$BCO. Thermal ellipsoids are drawn at the 50% probability level.

crystal structure containing ordered $(C_2F_5)_3$BCO molecules allowed for the determination of structural data with good accuracy. This is in contrast to the crystal structure of $(CF_3)_3$BCO, which was hampered by twinning and a low-temperature phase transition, resulting in large uncertainties and making difficult reliable comparisons. The environment about B comprises a shorter B−CO bond of 1.618(2)/1.625(2) Å than the three B−CF_2 bonds of 1.634(3) to 1.644(2) Å. The B−CO bond lengths in $(C_2F_5)_3$BCO and in gaseous $(CF_3)_3$BCO are the same within 3σ, and are one of the longest B−CO bonds. The long B−CO bond is paralleled by one of the shortest CO bond lengths with 1.109(2) Å observed so far. The CO bond length is significantly shorter than that of gaseous CO of 1.1281 Å.[11]

Structure of $(C_3F_7)_3BCO$: Tris(heptafluoropropyl)borane carbonyl crystallizes in the hexagonal space group $P6_3$ with the $(C_3F_7)_3$BCO on a crystallographic threefold rotational axis and the linear BCO moiety aligned along the c axis. A disorder was found with the BCO moiety oriented up (65%) and down (35%); only the values for the main component will be discussed. Similar to the pentafluoroethyl analogue, the heptafluoropropyl groups exhibit a propeller-like arrangement (Figure 10). The CO bond of 1.105(5) Å is comparable with that of $(C_2F_5)_3$BCO (1.109(2) Å). The main difference

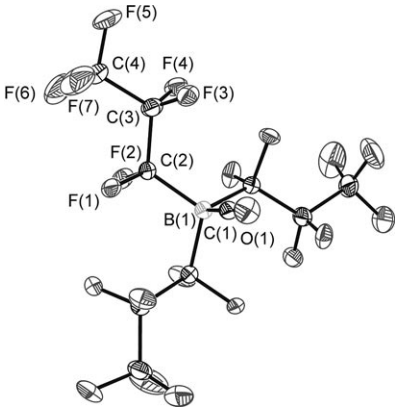

Figure 10. View of the main component of the X-ray crystal structure of $(C_3F_7)_3BCO$. Thermal ellipsoids are drawn at the 50% probability level.

lies in the B–CF_2 bonds, which are longer in $(C_3F_7)_3BCO$ than in $(C_2F_5)_3BCO$. The elongation of the B–CF_2 bonds is likely a consequence of the increased steric demand of the larger perfluoroalkyl groups.

Conclusion

The new boron carbonyls, $(C_2F_5)_3BCO$ and $(C_3F_7)_3BCO$, were prepared via known $[(R_f)_3BC{\equiv}CPh]^-$[6] and their oxidative cleavage of the triple bond forming the new $[(R_f)_3BCO{-}COPh]^-$ and $[(R_f)_3BCOOH]^-$. Subsequent reactions of the carboxylic acids with concentrated H_2SO_4 yielded the carbonyls for both perfluorinated side chains, proving that this new synthetic route to tris(perfluoroalkyl)borane carbonyls is of general application. The ordered crystal structure of $(C_2F_5)_3BCO$ at low temperature provides high-accuracy structural data for a perfluorinated borane carbonyl compound for the first time. The CO bond length and the CO stretching frequency is among the shortest and highest, respectively, evidencing the absence of π backdonation in the B–CO bond.

Experimental Section

Apparatus and chemicals: Volatile materials were manipulated in a glass vacuum line equipped with valves with PTFE stems (Young, London) and with capacitance pressure gauges (Type MKS Baratron 622 A). The ESI-neg. mass spectra were recorded by using a Bruker Daltonics micrOTOF instrument. DSC measurements of $Cs[(C_2F_5)_3BCO{-}COPh]$ and $K[(C_2F_5)_3BCOOH]{\cdot}H_2O$ were performed by using a Netzsch DSC 204. The acid-base titration for $K[(C_2F_5)_3BCOOH]$ and $K[(C_3F_7)_3BCOOH]$ were performed by using a Mettler–Toledo SevenMulti pH meter. C_2F_5I was obtained from ABCR. All standard chemicals and solvents were obtained from commercial sources.

$K[(C_2F_5)_3BCO\text{-}COPh]$ and $Cs[(C_2F_5)_3BCO{-}COPh]$: A solution of $KMnO_4$ (4.5 g) in water (300 mL) was stirred with $Cs[(C_2F_5)_3BCCPh]$ (4.0 g, 6.64 mmol) for five days at room temperature. Potassium sulfite (K_2SO_3) (ca. 12 g) was added under stirring and the solution was acidified by using dilute sulfuric acid until a colorless solution was obtained. The pH value was adjusted to 7–8 using K_2CO_3, and yellow $K[(C_2F_5)_3BCO{-}COPh]$ was extracted with diethyl ether (2×100 mL). Yield 3.3 g (6.18 mmol) 98%. $Cs[(C_2F_5)_3BCO{-}COPh]$ was precipitated from an aqueous solution of the potassium salt using CsI. M.p. 199°C; decomp 270°C (DSC measurement); ESI (negative-ion mode).: *m/z*: $C_{14}H_5{}^{11}BF_{15}O_2$ calcd: 501.0143; found: 501.026; $C_{14}H_5{}^{10}BF_{15}O_2$ calcd: 500.0179; found: 500.024; Raman lines of $Cs[(C_2F_5)_3BCO{-}COPh]$: $\tilde{\nu}$= 3197(1), 3168(1), 3084(44), 3041(2), 3017(3), 2982(2), 2930(8), 1713(3), 1667(66), 1642(11), 1616(sh), 1599(100), 1586(21), 1496(6), 1455(5), 1344(1), 1322(sh), 1312(7), 1267(18), 1239(3), 1203(6), 1187(8), 1167(12), 1135(8), 1092(6), 1068(3), 1041(sh), 1029(17), 1004(73), 992(4), 925(3), 913(1), 828(1), 810(2), 802(2), 756(sh), 740(29), 726(sh), 709(9), 669(1), 655(2), 634(6), 617(14), 607(5), 587(6), 534(1), 455(4), 438(4), 400(1), 372(6), 342(4), 326(sh), 318(5), 280(6), 268(3), 255(3), 238(6), 212(2), 204(1) cm^{-1}; IR absorptions of $Cs[(C_2F_5)_3BCO{-}COPh]$: $\tilde{\nu}$=3320(w), 3268(w), 3075(w), 1667(s), 1642(s), 1599(m), 1583(m), 1495(w), 1453(m), 1314(s), 1264(m), 1244(m), 1213(sh), 1204(svs), 1188(vs), 1181(sh), 1155(sh), 1145(vs), 1086(sh), 1053(vs), 1020(m), 1002 (w), 975(w), 935(w), 925(w), 913(w), 861(w), 848(s), 833(s), 815(w), 807(m), 800(sh), 757(m), 738(w), 729(s), 713(s), 683(s), 653(s), 629(vs), 619(w), 605(w), 582(s), 525(s), 434 cm^{-1} (m).

$K[(C_2F_5)_3BCOOH]{\cdot}H_2O$ and $K[(C_2F_5)_3BCOOH]$: To a solution of hypobromite, which was prepared from KOH (15 g) and Br_2 (5 mL) in water (280 mL), $K[(C_2F_5)_3BCO{-}COPh]$ (3 g, 5.55 mmol) was added. After the mixture had been stirred for 4 h at room temperature, potassium sulfite was added slowly until the yellow color of the hypobromite had disappeared. The pH value of the solution was adjusted to 4 by using KH_2PO_4/H_3PO_4, followed by the extraction of benzoic acid with $CHCl_3$ (2×100 mL). Extraction of the neutralized solution with diethylether furnished pure $K[(C_2F_5)_3BCOOH]{\cdot}H_2O$. Yield 2.2 g (4.7 mmol) 84%; loss of water of crystallization at 62°C (DSC); m.p. 120°C; decomp 170°C (DSC); ESI negative-ion mode: *m/z*: $C_7H^{11}BF_{15}O_2$ calcd: 412.9830; found: 412.9912; $C_7H^{10}BF_{15}O_2$ calcd: 411.9866; found: 411.9984; Raman lines of $K[(C_2F_5)_3BCOOH]$: $\tilde{\nu}$=3500(4), 3493(4), 1737(sh), 1726(13), 1716(9), 1329(8), 1315(10), 1302(sh), 1229(sh), 1214(9), 1203(9), 1182(6), 1146(11), 1124(6), 1083(7), 1068(6), 1033(3), 1008(5), 992(8), 811(1), 746-(100), 732(9), 676(8), 666(sh), 629(21), 598(sh), 590(19), 543(5), 515(3), 441(6), 434(sh), 378(28), 370(sh), 344(10), 318(18), 300(6), 283(19), 266(24), 242(11), 222(4), 174(10), 167(sh), 117(8) cm^{-1}; IR absorptions of $K[(C_2F_5)_3BCOOH]$: $\tilde{\nu}$=3500(m), 1740(sh), 1725(sh), 1719(s), 1325(sh), 1313(w), 1298(s), 1276(w), 1232(w), 1218(sh), 1201(m), 1193(m), 1162(s), 1147(vs), 1123(vs), 1081(m), 1062(vs), 1037(m), 1009(w), 989(w), 926(w), 911(sh), 901(m), 886(m), 866(w), 850(m), 837(s), 820(w), 811(m), 744(w), 730(s), 714(w), 684(sh), 667(vs), 629(w), 607(s), 598(s), 551(m), 531(m), 434 cm^{-1} (m); IR absorptions of $K[(C_2F_5)_3BCOOH]{\cdot}H_2O$: $\tilde{\nu}$=3671(m), 3589(w), 3030(w broad), 1701(w), 1659(s), 1623(w), 1328(sh), 1317(w), 1302(s), 1261(sh), 1246(sh), 1218(s), 1196(s), 1196(s), 1183(s), 1155(vs), 1146(sh), 1137(sh), 1081(s), 1068(s), 1060(s), 1037(m), 1014(w), 995(w), 937(sh), 928(m), 901(m), 869(w), 853(s), 848(sh), 821(w), 811(m), 750(w), 737(w), 721(sh), 714(vs), 695(sh), 676(sh), 629(m), 605(m), 600(sh), 583(w), 530 cm^{-1} (m).

$(C_2F_5)_3BCO$: After drying $K[(C_2F_5)_3BCOOH]{\cdot}H_2O$ (4.7 g, 10 mmol) in vacuo, 95% H_2SO_4 (ca. 20 mL) was added at 20°C to a 250 mL vessel connected to a vacuum line. The carbonyl that is immediately evolved was trapped at −60°C in a dynamic vacuum. Yield 3.8 g (9.6 mmol) 96%; m.p.: −28°C; b.p.≈107°C extrapolated; Raman lines of solid $(C_2F_5)_3BCO$: $\tilde{\nu}$=2263(100), 1332(16), 1236(7), 1228(10), 1203(9), 1171(8), 1097(17), 1051(2), 981(3), 884(3), 855(24), 824(4), 746(83), 721(3), 616(10), 606(11), 591(15), 534(8), 424(13), 370(29), 313(28), 264(11), 250(49), 229(17), 172(18), 149(4), 123(10) cm^{-1}; IR absorptions of gaseous $(C_2F_5)_3BCO$: $\tilde{\nu}$=2581(w), 2252(s), 2200(w), 1789(w), 1330(vs), 1249(vs), 1235(vs), 1229(sh), 1203(s), 1182(vs), 1159(sh), 1116(m), 1098(s), 1055(m), 1035(sh), 948(w), 902(w), 877(m), 856(m), 838(m), 823(m), 803(w), 744(w), 720(s), 705(w), 629(w), 613(m), 600(w), 589(sh), 534(m), 468(m), 454(w), 431(sh), 426(sh), 423(sh), 418 cm^{-1} (m).

$K[(C_3F_7)_3BCOOH]{\cdot}2H_2O$ and $K[(C_3F_7)_3BCOOH]$: The hydrate, $K[(C_3F_7)_3BCOOH]{\cdot}2H_2O$, has been prepared on a small scale according to the procedure used for the synthesis of $K[(C_2F_5)_3BCOOH]{\cdot}H_2O$. Waters of crystallization can be removed under dynamic vacuum at 50°C for 1 h.

IR absorptions of $K[(C_3F_7)_3BCOOH]\cdot 2H_2O$: $\tilde{\nu}=3679$(m), 3503(br/w), 2965(br/w), 1663(m), 1624(m), 1336(m), 1276(w), 1249(sh), 1209(vs), 1173(s), 1139(w), 1107(vs), 1060(sh), 1052(s), 1020(s), 962(m), 930(w), 904(w), 868(w), 809(m), 776(w), 747(w), 736(m), 708(vs), 675(w), 661(s), 626(w), 613(w), 609(w), 600(w), 560(m) 535(sh), 529(s), 497 cm^{-1} (w); IR absorptions of $K[(C_3F_7)_3BCOOH]$: $\tilde{\nu}=3568$(w), 3503(m), 1723(m), 1705(m), 1338(s), 1204(vs), 1188(vs), 1170(sh), 1140(sh), 1128(w), 1106(vs), 1097(s), 1063(sh), 1052(s), 1045(sh), 1015(w), 977(w), 960(m), 928(w), 917(w), 904(m), 867(m), 840(sh), 834(m), 799(m), 794(sh), 785(sh), 741(w), 729(m), 718(sh), 714(s), 695(m), 682(s), 673(sh), 652(s), 637(s), 628(sh), 608(w), 582(w), 566(m), 533(m), 527(sh), 492 cm^{-1}(w); ESI negative-ion mode: m/z:$C_{10}H^{11}BF_{21}O_2$ calcd: 562.9734; found: 562.9742,$C_{10}H^{10}BF_{21}O_2$ calcd: 561.9770; found: 561.9776.

$(C_3F_7)_3BCO$: The carbonyl was prepared according to the general procedure used for the synthesis of $(C_2F_5)_3BCO$. Tris(heptafluoropropyl)borane carbonyl was trapped at −20 °C after being generated by reaction with concentrated sulfuric acid. M.p.: +5 °C, vapor pressure at 20 °C ≈1 mbar; IR absorptions of gaseous $[(C_3F_7)_3BCO]$: $\tilde{\nu}=2249$(s), 2197(w), 1341(s), 1279(s), 1245(vs), 1230(vs), 1203(s), 1183(s), 1169(sh), 1123(s), 1117(sh), 1103(s), 1085(m), 1062(m), 988(sh), 970(m), 960(sh), 902(w), 856(w), 818(w), 787(w), 768(w), 741(w), 722(s), 714(s), 704(m), 694(sh), 674(w), 661(m), 646(m), 630(sh), 586(sh), 573(w), 565(sh), 532(m), 509(w), 454(m), 442 cm^{-1} (m).

Vibrational spectroscopy: The FT-IR spectra of $Cs[(C_2F_5)_3BCO{-}COPh]$, $K[(C_2F_5)_3BCOOH]\cdot H_2O$, $K[(C_2F_5)_3BCOOH]$, $K[(C_3F_7)_3BCOOH]\cdot H_2O$, and $K[(C_3F_7)_3BCOOH]$ were recorded as neat solids by using a Bruker Tensor 27 FT IR spectrometer equipped with a diamond ATR accessory (Harrick MVP Star). The spectra were acquired in 32 scans at a resolution of 2 cm^{-1}.

The gas-phase IR spectra of $(C_2F_5)_3BCO$, $(C_3F_7)_3BCO$ and their decomposition productions were recorded by using a Bruker Vector 22 FT IR spectrometer in an IR gas cell with an optical path length of 200 mm and 0.6 cm thick Si windows. The gas cell was contained in the sample compartment of the spectrometer and directly connected to a vacuum manifold. Spectra were acquired for the range of $\tilde{\nu}=4000$–400 cm^{-1} with an optical resolution of 2 cm^{-1} and 32 scans.

The decomposition kinetics of $(C_2F_5)_3BCO$ was studied by using a Bruker Tensor 27 FT IR spectrometer using an IR gas cell with CaF_2 windows and a thermostated jacket. The temperature of the circulated water was regulated by a Julabo F25ME thermostate and the temperature of the circulated water was measured behind the IR cell. Spectra of the gas-phase samples were acquired with an initial pressure of 4 mbar for the range of 4000–900 cm^{-1} with an optical resolution of 2 cm^{-1} and 16 scans. The half life of $(C_2F_5)_3BCO$ was redetermined at 20 °C with a 1:10 carbonyl : N_2 dilution and was found to be essentially the same as for the neat gas.

The Raman spectra of $Cs[(C_2F_5)_3BCO{-}COPh]$, $K[(C_2F_5)_3BCOOH]$, $(C_2F_5)_3BCO$ were recorded by using a Bruker-Equinox 55 FRA 106/S FT-Raman spectrometer using the 1064 nm excitation of a Nd:YAG laser (200 mW); 1500 scans were recorded at a resolution of 3 cm^{-1} ($Cs[(C_2F_5)_3BCO{-}COPh]$ and $K[(C_2F_5)_3BCOOH]$). For the low-temperature Raman measurement of $(C_2F_5)_3BCO$, the samples were condensed onto a copper finger at −196 °C in high vacuum; 36 scans were recorded at a resolution of 2 cm^{-1} ($(C_2F_5)_3BCO$).

Nuclear magnetic resonance spectroscopy: Proton, ^{13}C, and ^{19}F NMR spectra were recorded by using a Bruker ARX 400 spectrometer operating at 400.13, 100.61, and 376.5 MHz, respectively. Boron-11 NMR spectra were recorded by using a Bruker AC 250 spectrometer operating at 80.17 MHz. The NMR signals were referenced against the solvent signal of [D_6]acetone as internal standards (^1H: $\delta_H=2.03$, ^{13}C: $\delta_C=30.50$) and against $CFCl_3$ and $BF_3\cdot OEt_2$ as external standards for ^{19}F and ^{11}B, respectively. The samples of neat $(C_2F_5)_3BCO$ and $(C_3F_7)_3BCO$ were prepared in a sealed 4 mm glass tube, which was inserted into a standard 5 mm NMR tube for NMR measurements at −20 and 6 °C, respectively.

X-ray crystal structure determination:

Crystal growth and crystal mounting: Crystals of $K[(C_2F_5)_3BCO{-}COPh]$ were grown from diethyl ether upon vapor diffusion of CH_2Cl_2. Crystals of $K[(C_2F_5)_3BCOOH]\cdot H_2O$ were grown from a mixture of diethyl ether and CH_2Cl_2 upon slow evaporation of the solvent mixture. Crystals of $(C_2F_5)_3BCO$ and $(C_3F_7)_3BCO$ were grown by sublimation at approximately −40 and −10 °C, respectively, in a sealed evacuated glass tubes. The glass tubes containing crystals of $(C_2F_5)_3BCO$ and $(C_3F_7)_3BCO$ were cut under in a cold nitrogen stream (≈−70 °C) while maintaining the sample at −80 °C, and the colorless crystals were quickly transferred into a trough cooled by a flow of cold nitrogen. A crystal of $(C_2F_5)_3BCO$ and $(C_3F_7)_3BCO$ having the dimensions $0.249\times0.159\times0.048$ and $0.234\times0.051\times0.039$ mm, respectively, were selected at approximately −70 °C under the microscope. The crystals were picked with a mounted CryoLoop (Hampton Res.) with a magnetic base using a CrystalWand (Hampton Res.) as a handle. The crystal was transferred to the goniometer using CryoTongs (Hampton Res.) that had been immersed in liquid nitrogen.

Collection and reduction of X-ray data: The crystal of $K[(C_2F_5)_3BCO{-}COPh]$ (*I2/a* modification) was centered by using a Bruker P4-SMART diffractometer equipped with a SMART 1 K charge-coupled device (CCD) area detector (using the program SMART).[12] For the data collection the Mo source emitting graphite-monochromated $Mo_{K\alpha}$ radiation ($\lambda=0.71073$ Å) was used. Processing was carried out by using the program SAINT,[13] which applied Lorentz and polarization corrections to three-dimensionally integrated diffraction spots. The program SADABS[14] was used for the scaling of diffraction data, the application of a decay correction, and an empirical absorption correction based on redundant reflections.

Crystals of $K[(C_2F_5)_3BCO{-}COPh]$, $K[(C_2F_5)_3BCOOH]\cdot H_2O$, $K[(C_3F_7)_3BCOOH]\cdot 2H_2O$, $(C_2F_5)_3BCO$, and $(C_3F_7)_3BCO$ were centered on a Oxford Diffraction Gemini E Ultra diffractometer, equipped with a 2 K×2 K EOS CCD area detector, a four-circle kappa goniometer, sealed-tube Enhanced (Mo), and the Enhanced Ultra (Cu) X-ray sources, and an Oxford Instruments Cryojet. For the data collection the Mo source emitting graphite-monochromated $Mo_{K\alpha}$ radiation ($\lambda=0.71073$ Å) was used. The diffractometer was controlled by the CrysAlis^{Pro} Graphical User Interface (GUI) software.[15] Diffraction data collection strategies for $K[(C_2F_5)_3BCO{-}COPh]$, $K[(C_2F_5)_3BCOOH]\cdot H_2O$, $K[(C_3F_7)_3BCOOH]\cdot 2H_2O$, $(C_2F_5)_3BCO$, and $(C_3F_7)_3BCO$ were optimized with respect to complete coverage and consisted of eight, four, seven, six, and, three ω scans with a width of 1°, respectively. The data collection was carried out at −123 °C in a 1024×1024 pixel mode using 2×2 pixel binning. Processing of the raw data, scaling of diffraction data and the application of an empirical absorption correction was completed by using the CrysAlis^{Pro} program.[15]

Solution and refinement of the structure: The solutions were obtained by direct methods which located the positions of the non-hydrogen atoms. The final refinement was obtained by introducing anisotropic thermal parameters and the recommended weightings for all of the atoms. The positions of the hydrogen atoms were found in the difference map and their position was refined. The maximum electron densities in the final difference Fourier map were located near the heavy atoms. The $P2_1/n$ polymorph of $K[(C_2F_5)_3BCO{-}COPh]$ was refined with a 28.9% twin component according to the twin law (1 0 0, 0 −1 0, 0 0 −1). The crystal structure of $K[(C_3F_7)_3BCOOH]\cdot 2H_2O$ was hampered by variable degrees of disorder of the heptafluoropropyl side chains and two water molecules. In the final structure, the disorder of two side chains was modeled. Residual density indicated small degrees (<10%) of disorder for other side chains and split position for two water molecules (≈10%). Modeling of the additional disorder proved to be difficult and did not result in improved R values and uncertainties in bond lengths and angles. All calculations were performed using the SHELXTL-plus package for the structure determination and solution refinement and for the molecular graphics.[16]

CCDC-763012 ($K[(C_2F_5)_3BCO{-}COPh]$, $P2_1/n$), CCDC-763014 ($K[(C_2F_5)_3BCO{-}COPh]$, *I2/a*), CCDC-763009 ($K[(C_2F_5)_3BCOOH]\cdot H_2O$), CCDC-763011 ($K[(C_3F_7)_3BCOOH]\cdot 2H_2O$), CCDC-763010 ($(C_2F_5)_3BCO$), and CCDC-763014 ($(C_3F_7)_3BCO$) contain the supplementary crystallographic data for this paper. These data can be obtained free of charge

from The Cambridge Crystallographic Data Centre via www.ccdc.cam.ac.uk/data_request/cif.

Acknowledgements

We are indebted to the Fonds der Chemischen Industrie and the Merck Company, Darmstadt for financial support. M.G. acknowledges the University of Lethbridge for granting a study leave. We thank Prof. Dr. R. Eujen for his help with the acquisition of the low-temperature NMR spectra and Dr. J. Hübner is acknowledged for the DSC measurements and the acid–base titrations.

[1] A. Terheiden, E. Bernhardt, H. Willner, F. Aubke, *Angew. Chem.* **2002**, *114*, 823–825; *Angew. Chem. Int. Ed.* **2002**, *41*, 799–801.
[2] M. Finze, E. Bernhardt, A. Terheiden, M. Berkei, H. Willner, D. Christen, H. Oberhammer, F. Aubke, *J. Am. Chem. Soc.* **2002**, *124*, 15385–15398.
[3] M. Finze, E. Bernhardt, H. Willner, *Angew. Chem.* **2007**, *119*, 9340–9357; *Angew. Chem. Int. Ed.* **2007**, *46*, 9180–9196.
[4] G. Pawelke, H. Bürger, *Coord. Chem. Rev.* **2001**, *215*, 243–266.
[5] M. Finze, E. Bernhardt, M. Zähres, H. Willner, *Inorg. Chem.* **2004**, *43*, 490–505.
[6] E. Bernhardt, D. J. Bauer, M. Köckerling, G. Pawelke, *Z. Anorg. Allg. Chem.* **2007**, *633*, 947–954.
[7] T. J. Brice, J. D. LaZerte, L. J. Hals, W. H. Pearlson, *J. Am. Chem. Soc.* **1953**, *75*, 2698–2702.
[8] C. Harzdorf, J. N. Meußdoerffer, H. Niederprüm, M. Wechsberg, *Ann. Chemie* **1973**, *1*, 33–39.
[9] D. Bejan, H. Willner, N. Ignatiev, C. W. Lehmann, *Inorg. Chem.* **2008**, *47*, 9085–9089.
[10] E. Pretsch, P. Bühlmann, M. Badertscher, *Structure Determination of Organic Compounds*, Springer, Berlin, **2009**, pp. 131–132.
[11] K. P. Huber, G. Herzberg, *Molecular Spectra and Molecular Structure. Constants of Diatomic Molecules*, van Nostrand, New York, **1979**.
[12] SMART, Bruker Molecular Analysis Research Tool, v. 5.054, Bruker-AXS, Madison, Wisconsin, **2007**.
[13] SAINT, data reduction and correction program, v. 7.46, Bruker-AXS, Madison, Wisconsin, **2007**.
[14] SADABS, Bruker/Siemens Area Detector Absorption Correction Program, Bruker-AXS, G. M. Sheldrick, Madison, Wisconsin, **2007**.
[15] CrysAlisPro, Version 1.171.33.34d, Oxford Diffraction Ltd., **2009**.
[16] SHELXTL97, G. M. Sheldrick, University of Göttingen, Göttingen, **1997**.

Received: January 26, 2010
Published online: May 12, 2010

